STRUCTURAL OPTIMIZATION OF COMPOSITE PANELS CONSIDERING THE MANUFACTURING PROCESS

Moo Sun KIM*,, Woo Il LEE*, Woo Suck HAN**, Alain VAUTRIN****
[Moo Sun KIM]: moosun1@snu.ac.kr
*** School of Mechanical and Aerospace Engineering, Seoul National University, Seoul 151-741, South Korea, ** Mechanical and Materials Engineering Department, Ecole Nationale Supérieure des Mines de Saint-Etienne, 42023 Saint-Etienne,**

Keywords: *compression molding, fiber separation, fiber orientation, mechanical properties, thickness optimization*

Abstract

The main goal of this study is to optimize processing conditions and structural design to improve the mechanical performance of composite structure manufactured by compression molding process. As the preliminary preparation of optimization, we developed a processing simulation program to predict fiber states by CV/FEM and a structural analysis program by DRM element to consider simultaneously the mechanical requirements and the manufacturing process. For simple geometries, effects of processing conditions on the mechanical properties were verified. A plate with variable thickness was also investigated. Optimal structural design considering processing conditions was searched by applying Box's complex method.

1 Introduction

Compression molding is the manufacturing process by compressing precharge in the mold. One of the advantages of this manufacturing process is relatively short process cycle suited for mass production for industries such as automobile manufacturing. Also, mechanical properties of the final product are good in general. In many cases, sheet molding compound (SMC) in the form of thin plate is used for compression molding. The charging process gives great influences on the mechanical properties of the final product. Fiber states, such as fiber volume fraction and fiber orientation can change the mechanical properties. Non-uniform distribution of fiber volume fraction, due to fiber separation or change in fiber orientation, gives rise to non-uniform mechanical properties in the final product. Therefore, accurate prediction of fiber states conditions is crucial to optimization of process and thus in obtaining the required mechanical characteristics. There are two models suggested for the flow analysis of compression molding process: the generalized Hele-Shaw (GHS) model [1] and the Barone-Caulk model [2]. In this study, the GHS model was adopted for 2-dimensional flow analysis. The CV/FEM (Control Volume FEM) method was employed for the numerical scheme. Fiber separation is caused by the fiber-matrix and fiber-fiber interaction [3, 4, 5]. Along with the non-uniformity in fiber volume fraction, fiber orientation distribution is one of main causes for uneven properties in the product. As the methods to represent the state of fiber orientation, the fiber orientation distribution function [6] or the fiber orientation tensors [7] can be used. In order to predict the mechanical properties of short-fiber composite, properties of unidirectional composite was estimated first. Halpin-Tsai equation is the most popular model to predict the properties of short-fiber composites and used to estimate the mechanical properties of unidirectional composite [8]. Properties of the short fiber composite then are taken as an average of the unidirectional properties over all direction. The final fiber orientation tensors obtained from the processing simulation are used for the "orientation averaging" [7]. A series of triangular elements has been introduced based on Reissner-Mindlin assumptions. As the robust triangular elements for thin and thick plate, DST (Discrete Shear Triangle) element [9] and DRM (Discrete

Reissner-Mindlin) element [10] are suggested. To search the best mechanical properties to be induced from the process, precharge conditions (location and dimension) and structural design (thickness) can be considered. Among optimization methods, direct search method doesn't require gradient information and thus is suited for a nonlinear constraint problem considered here. In this study, Box's complex method [11] is employed.

2 Modeling for flow and fiber states

2.1 Flow modeling

For the GHS model, it is assumed that the inertia of the material is negligible, the material is incompressible. Due to small thickness, only the variation of shear stress in z-direction is considered in the momentum equation. The flow velocity is defined as the in-plane velocity averaged through the thickness of material. With the above assumptions, from the continuity equation and momentum equation, governing equation can be obtained as follows [1].

$$\frac{\partial}{\partial x}\left(\frac{S}{h}\frac{\partial P}{\partial x}\right)+\frac{\partial}{\partial y}\left(\frac{S}{h}\frac{\partial P}{\partial y}\right)=\frac{\dot{h}}{h} \qquad (1)$$

where $P, h, \dot{h}$ are pressure, thickness and compression speed, respectively and S is defined as flow conductance.

2.2 Fiber separation and orientation modeling

2.2.1 Fiber separation

Due to interaction between the fibers, reinforcing fibers may move at different speed from the main flow. Due to the relative velocity between the fibers and the main flow, initial homogeneous fiber volume fraction in precharge may become non-homogeneous, causing non-uniformity in the final mechanical properties. The network force, F_{nw}, which is frictional force acting on a fiber tow from contact with neighboring fiber tows, acts as a resisting force and thus gives rise to relative motion of fibers. Relative velocity of matrix and fiber, u_s, is defined as

$$u_s = u_c - u_f \qquad (2)$$

where u_c is the matrix velocity and u_f is the fiber velocity. It can be assumed that the drag force on fiber tows by the resin flow is balanced with the frictional force on a fiber tows. Therefore, the relative velocity can be determined by using the equivalence of drag force and network force. The network force can be written as

$$F_{nw}=\frac{1}{2}C_D\,\rho_m\,u_s^2\,A_p \qquad (3)$$

where C_D, ρ_m and A_p represent the drag coefficient, the density of matrix and the area where drag force is acting, respectively. Network force, F_{nw}, is defined as the resultant of friction forces (Fig. 1.) acting on the fiber at different contact points with surrounding fibers. This difference in friction force is due to the pressure variation acting on the fiber. Network force can be presented as the following.

$$F_{nw}=\kappa\left(r_{up}\int_{x_o-l_f/2}^{x_o}p(s)\,D_f\,ds-r_{dn}\int_{x_o}^{x_o+l_f/2}p(x)\,D_f ds\right) \qquad (4)$$

where κ is a proportionality constant, r_{up} and r_{dn} are correction parameters, l_f is fiber length, and D_f is fiber diameter.

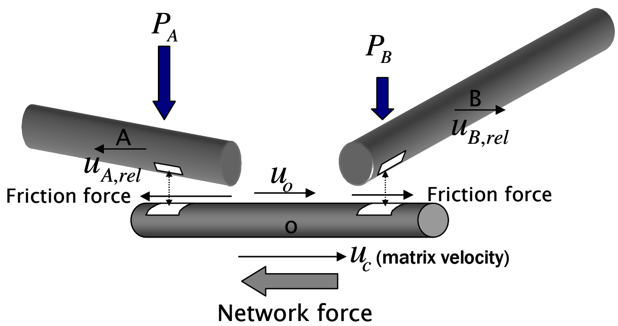

Fig. 1. Scheme of friction force by contacts between fibers

2.2.2 Fiber orientation

Advani et al.[7] proposed a method to represent fiber orientation using orientation tensors. A compact and general description of fiber orientation state is provided by the tensors defined as the following:

$$a_{ij}=\oint p_i p_j \psi(p)dp \qquad (5)$$

$$a_{ijkl}=\oint p_i p_j p_k p_l \psi(p)dp \qquad (6)$$

where unit vector p_i for two-dimensional orientation is defined as $p_1 = \cos\theta,\ p_2 = \sin\theta$. Note that a_{ij} is symmetric and its trace is equal to unity. The advantage of using the tensor representation is that only a few numbers are required to describe the orientation state at any point in space. For planar orientations there are four components of a_{ij}, but only two are independent. Folgar and Tucker's equation of single fiber motion in a concentrated suspension [14] can be combined with the equation of continuity to produce an equation of change for the probability distribution function and/or the orientation tensor. The result for second-order orientation tensors is

$$\frac{Da_{ij}}{Dt} = -\frac{1}{2}(\omega_{ik}a_{kj} - a_{ik}\omega_{kj}) + \frac{1}{2}\lambda(\dot{\gamma}_{ik}a_{kj} + a_{ik}\dot{\gamma}_k - 2\dot{\gamma}_{kl}a_{ijkl}) + 2C_I\,\dot{\gamma}(\delta_{ij} - \alpha a_{ij}) \tag{7}$$

where δ_{ij} is the unit tensor and α is equal to 3 for three-dimensional orientation and to 2 for planar orientation. ω_{ij} and $\dot{\gamma}_{ij}$ are the vorticity and the rate of deformation tensors, respectively.

2.3 Numerical analysis

As process material fills the mould, calculation domain changes. For the analysis of fluid flow in this study, the fixed grid method is applied. For definition of the calculation domain, volume of fluid (VOF) method, which uses the volume fraction of each control volume, is used. To calculate more exact pressure distribution in flow front elements, the FINE method [12] is applied. From the pressure information of each node, velocity can be computed at the centroid of an element. Then the velocity of one node is evaluated by the average of those values computed at its surrounding elements.

Fiber volume fraction can be computed by integration of mass conservation of fiber for control volume by assuming that the fiber content and the rate of fiber content change are constant.

$$\frac{\partial\phi}{\partial t}V_{c.v} + \int_{c.s}\phi\vec{v}\cdot\hat{n}\,d\Gamma = -\frac{\dot{h}}{h}\phi V_{c.v} \tag{8}$$

$$\phi_{new} = \phi_{old} - \left(\frac{\int_{\Gamma}\phi_{old}\overline{v}_f\cdot\hat{n}\,d\Gamma}{V_{c.v}} + \frac{\dot{h}}{h}\phi_{old}\right)\Delta t \tag{9}$$

where $\overline{v}_f$ is the fiber velocity.

When evaluating fiber orientation tensors at each nodes (Eq. 7), hybrid closure approximation [7] is used as closure approximation of 4th order tensors to 2nd order tensors.

3 Structural analysis

By using fiber volume fraction and fiber orientation tensors obtained from the processing simulation, mechanical properties of composite structure can be estimated.

First, properties of unidirectional material, is estimated using Halpin-Tasi equation [8]. Unidirectional properties thus obtained are averaged using the fiber volume fraction and fiber orientation distribution to compute the mechanical properties of final product.

For structural analysis, flat element was employed. Typical flat element is subject to plane stress and plate bending action. Therefore, stiffness matrix is formed by assembling the plane stress and plate bending stiffness matrices. Also, plate bending stiffness matrix is composed of two different stiffness matrices from bending moments and transverse shear forces.

In this paper, DRM element is used for plate bending problem. For three-node DRM element, the rotation, θ, and transverse displacement, w, are interpolated within the element as

$$\theta = \sum_{i=1}^{3}L_i\overline{\theta}^i + \sum_{j=1}^{3}4L_iL_j\Delta\overline{\theta}^k e_k \qquad w = \sum_{i=1}^{3}L_i\overline{w}^i \tag{10}$$

where $\Delta\overline{\theta}^k$ is a hierarchical tangential rotation parameter at the element mid-side, L_i is the standard area coordinates and the components of e_k are the direction cosines of the sides on which L_k=0.

4 Optimization of structural thickness and processing conditions

As the flow distance to fill the mold is shorter and the thickness of precharge is larger, fiber volume fraction distribution becomes more even. If there were no velocity gradient within the flow, the initial isotropic fiber orientation can be kept unchanged. However, considering the unavoidable fiber states changes during filling, best available fiber states have to found to meet the specified loading condition on a structure. Therefore processing conditions such as precharge location and dimension are considered as design variables to optimize mechanical properties. As well as the processing conditions, structural design parameter (e.g. structure thickness) is another dominant design variable to influence structural properties.

In this study, effects of precharge location and dimensions on structural properties are verified through the case studies and the optimal structure thickness is searched by Box's complex method.

4.1 Box's complex method

Box's complex method is one of the direct search methods to optimize problems with inequality constraints. It is straightforward to implement and is suited for the nonlinear problem considered in this study [13].

Box's complex method is a local minimization method. Inequality constraints define a convex region in this method and convexity of the feasible solution region must be ensured. Box's complex method scheme is shown in Fig. 2.

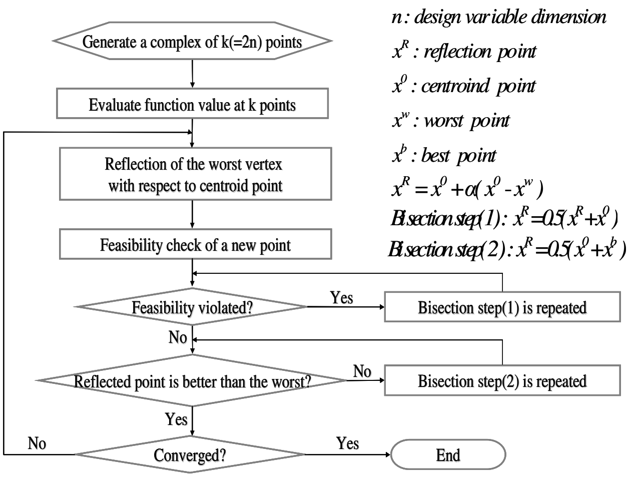

Fig. 2. Box's complex method scheme

4.2 Case study

As an example to demonstrate the influence of precharge location and dimension to structural properties, consider a rectangular plate under the loading condition as in Fig. 3. Maximum deflection can be calculated for the fiber states obtained for different processing conditions. Material properties of precharge and processing conditions for simulation are listed in Table. 1.

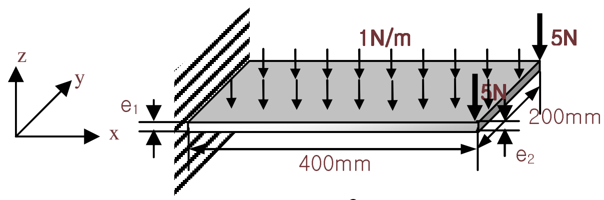

$$e_1 = e_2 = 3mm$$

Fig. 3. Geometry of clamped plate and loading conditions

Table. 1. Precharge material properties and processing conditions

Initial fiber volume fraction	30%
Fiber length	25mm
Compression speed	1mm/sec
Viscosity	500 Pa-sec
Initial fiber orientation	Random
Fiber tensile modulus	72.5e9Pa
Fiber shear modulus	30e9Pa
Fiber Poisson ratio	0.2
Resin tensile modulus	2.62e9Pa
Resin shear modulus	0.984e9Pa
Resin Poisson ratio	0.32

To verify the effect of precharge location, two cases are considered. In the first case, precharge is located on the left side of the mold while in the other case precharge is on the right side (Fig. 4).

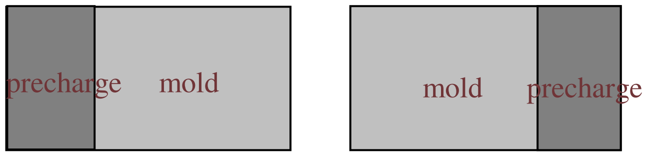

(a) (b)

Fig. 4.(a)Left-located precharge (30% covered mold)
(b) Right_located precharge (30% covered mold)

Resulting mechanical properties are compared with the case of homogeneous fiber volume fraction and isotropic fiber orientation as in Fig. 5.

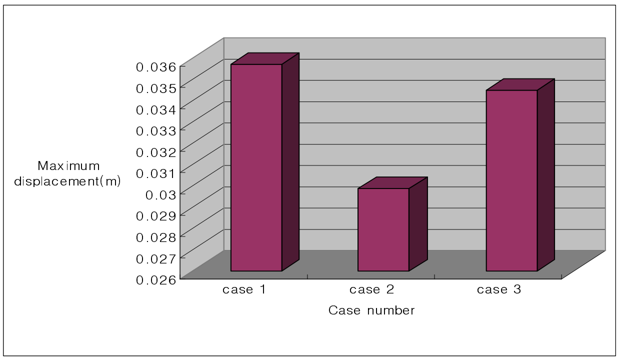

Fig. 5. Maximum displacement of structure
Case 1: homogeneous fiber volume fraction and isotropic fiber orientation
Case 2: left-located precharge condition
Case 3: right-located precharge condition

In case of left-located precharge, fiber separation phenomenon leaves more fibers than average in the clamped end where the bending moment is largest and deflection becomes small. Moreover, fibers tend to align with the flow direction resulting in higher stiffness along the flow direction. This coincides with the loading direction and thus deflection becomes minimal. In case of right-located precharge, although it shows the least fiber volume fraction in clamped end, the fibers align with the loading direction to have higher stiffness than the plate with homogeneous and isotropic fiber states.

In the second example, a plate with a hole is considered for different precharge locations and dimensions. As shown in Fig. 7, precharge is located in the mold at three different locations. Resulting displacements are compared in Fig. 8.

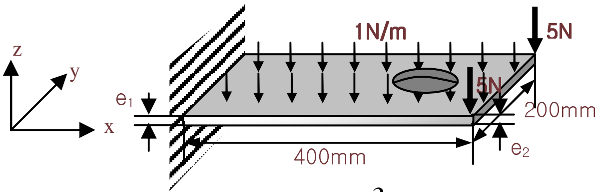

$e_1 = e_2 = 3mm$

Fig. 6. Geometry of plate with a hole

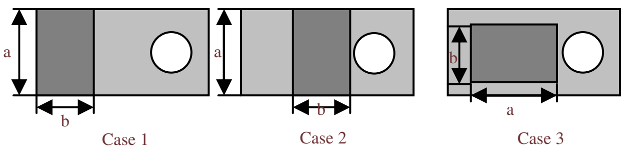

Fig. 7. Precharge location and dimension
(a= 200mm, b=120mm)

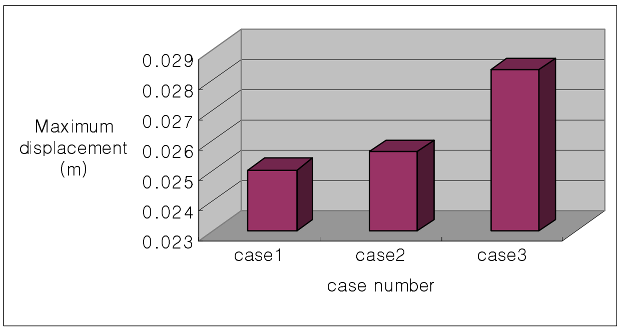

Fig. 8. Maximum displacement of structure

It shows that the left-located precharge is the best solution. However, even if the precharges are located at the same position, depending on their dimension, effects on the structural properties are different.

4.3 Numerical example

For application of proposed optimization scheme, a rectangular plate is considered under the loading condition as shown in Fig. 9. For thickness optimization, longitudinal section of the structure is considered to have varying thickness. For example, if the longitudinal section thickness is allowed to change in a quadratic form, possible form for the least displacement under the loading condition is one of the shapes shown in Fig. 10.

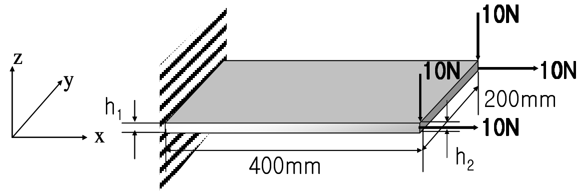

Fig. 9. Geometry of clamped plate and loading conditions

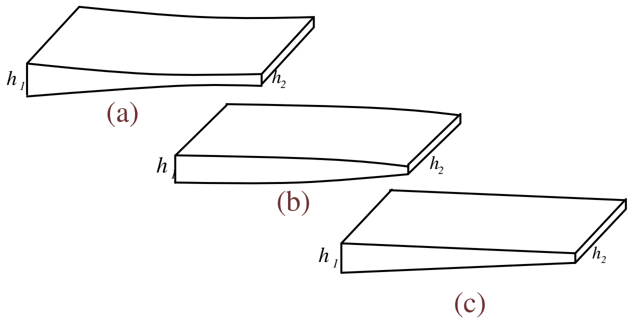

Fig. 10. (a) Concave (b) Convex and (c) Linear form

It is assumed that the structure weights are constant (i.e. constant precharge weight) and precharge location and dimension is fixed as shown in Fig. 11.

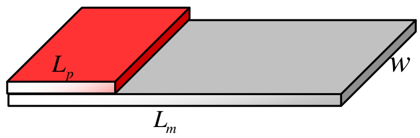

$L_p = 0.3L_m$

Fig. 11. Precharge location and dimension

As the longitudinal shape of the section is varied in a quadratic form, it can be written as $ax^2 + bx$, in which a and b are design variables to determine. Other variables to be decided are side thicknesses h_1 and h_2 . Therefore we can define design variable vector $\bar{x}$ as follows

$$\bar{x} = \bar{x}(a, b, h_1, h_2) \qquad (11)$$

The objective function is defined as

$$\begin{aligned} & f(\bar{x}(a,b,h_1,h_2)) = \frac{1}{d}, \quad d: displacement \\ & subject\ to\ -\frac{b}{2a} \le 0\ or\ -\frac{b}{2a} \le L_m \\ & and\ constant\ weight\ W \\ & (i.e. constant\ volume\ V) \end{aligned} \qquad (12)$$

We define new design variable, ε as the difference between h_1 and h_2. Using this definition, some of design variables can be converted as

$$b = \frac{\varepsilon - aL_m^2}{L_m}, \quad \varepsilon = h_1 - h_2$$
$$h_1 = \frac{V/w}{L_m} + \frac{1}{2}\varepsilon - \frac{1}{6}aL_m^2 \qquad (13)$$

Previous objective function with 4 design variables (Eq.12) is changed into the following function with two design variables

$$f(\bar{x}(a,\varepsilon)) = \frac{1}{d}$$
$$subject\ to\ -\frac{1}{L_m^2} \le \frac{a}{\varepsilon} \le \frac{1}{L_m^2} \qquad (14)$$

Optimized thickness is searched by Box's complex method. Computational process of finding optimal design variables and maximum displacement for both cases of compression molded plate and homogeneous and isotropic plate are compared in Fig. 12.

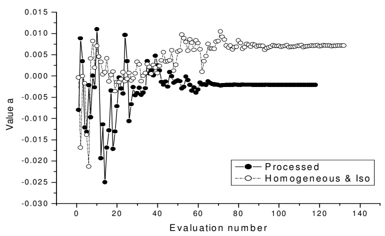

(a) design variable a

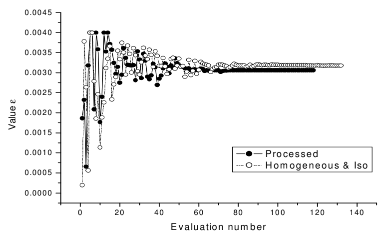

(b) design variable ε

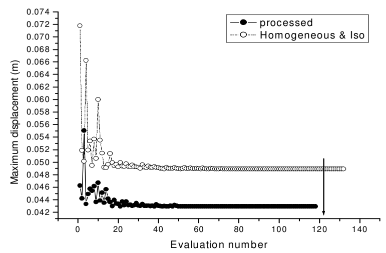

(c) maximum displacement d

Fig. 12. Computational process toward the optimum

As shown in the figure, a has different values for each case. For compression molded plate, a has a negative value indicating that thickness has concave profile. On the other hand, homogeneous and isotropic plate has positive a and thus the thickness profile is convex. It is found that although an magnitude of variation in a and ε of the compression molded plate is larger in the early evaluations, most of displacement is less than the homogeneous and isotropic plate.

Results are compared in Table.2. It is found that the compression molded plate shows less displacement than the homogeneous and isotropic plate by 13%.

Table.2. Optimized results

	a	ε	$d(m)$
Compression molded plate	-0.0019	0.00307	0.0429
Homogeneous and isotropic plate	0.0072	0.00317	0.0490

5 Conclusions

To investigate the influence of processing conditions of compression molding on structural properties of finished products, an optimization scheme has been proposed. Considering processing conditions, optimal structural design was researched by effectively defining design variables and applying a robust optimization technique. As other design variables, precharge location and dimension can be considered simultaneously. It forms an optimization problem as combinatorial and it demands the global optimization technique such as genetic algorithm. Case studies with simple shape mold and specified loading conditions were performed to evaluate the proposed method.

These optimization methodologies will help engineers to design products manufactured by compression molding through giving a guideline to determine the processing conditions and design parameters of structures, and eventually to save the development cost.

Acknowledgements

The authors of this paper would like to thank Ministry of Commerce, Industry and Energy for sponsoring this research through the wind turbine core technology research center, and the Korea Science and Engineering Foundation (KOSEF) for sponsoring this research through the SRC/ERC Program of MOST/KOSEF (R11-2005-065)

References

[1] Folgar F. and Tucker III C.L. "A Model of Compression Mold Filling". *Polymer Engineering and Science*, Vol.23, No.2, pp 69-73, 1983.

[2] Barone M.R. and Caulk D.A. (1986). "A model for the flow of a chopped fiber reinforced polymer compound in compression molding". *Journal of Applied Mechanics*, Vol.**53**, pp 361-371, 1986.

[3] Yoo, Y.E. "*A Study on the analysis of compression molding process of composite material structures*". Ph.D.Thesis, Seoul National University, Seoul, 1997.

[4] Hojo H., Nagatsuka C., Kim E.G. and Tamakawa K. "Separation of matrix and fibers during molding of long fiber-reinforced thermoplastics". *Proceedings of the Third Japan-U.S Conference on Composite Materials*, pp 605-612, 1986.

[5] Hojo, H., Kim E.G., Yaguchi H. and Onodera T. "Simulation of compression molding with matrix-fiber separation and fiber orientation for long fiber-reinforced thermoplastics". *Intern.Polymer Processing III*, pp 54-61, 1988.

[6] Jackson W.C., Tucker C.L. and Advani S.G. "Predicting the orientation of short fibers in thin compression moldings". *Journal of Composite Materials*, Vol.**20,** pp 539-557, 1986.

[7] Advani, S.G. and Tucker III C.L. "The use of tensors to describe and predict fiber orientation in short fiber orientation in short fiber composite". *Journal of Rheology*, Vol.31, No. 8, pp 751-784, 1987.

[8] Halpin, J.C. and Kardos, J.L. "The Halpin-Tsai Equation: A Review". *Polymer Engineering and Science*, Vol.16, No.5, pp 344-352, 1976.

[9] Batoz J.L. and Lardeur P. "A discrete shear triangular nine d.o.f. element for the analysis of thick to very thin plates". *International Journal for Numerical Methods in Engineering*, Vol.28, pp 533-560, 1989.

[10] Zienkiewicz O.C., Taylor R.L., Papadopoulos P. and Onate E. "Plate bending elements with discrete constraints: new triangular elements". *Computers & Structures***,** Vol.35, No.4, pp 505-522, 1990.

[11] Box M.J. "A new method of constrained optimization and a comparison with other methods". *Comput Journal,* Vol.8, pp 42-52, 1965.

[12] Kang, M.K. and Lee W.I. "A flow-front refinement technique for the numerical simulation of the resin-transfer molding process". *Composite Science and Technology*, Vol.59, pp 1663-1674, 1999.

[13] Robert M.L., Virginia T. and Michael W.T. "Direct search methods: then and now". *Journal of Computational and Applied Mathematics*, Vol.124, pp 191-207, 2000.

[14] Folgar F. and Tucker III C.L. "Orientation behavior of fibers in concentrated suspensions". *J. Reinf. Plast. Compos*, Vol.**3**, pp 98-119, 1984.